Comparative Analysis of Transmission Power Level and Packet Size Optimization Strategies for WSNs

Huseyin Ugur Yildiz, *Member*, *IEEE*, Sinan Kurt, and Bulent Tavli, *Senior Member*, *IEEE*

***Abstract*—Wireless Sensor Networks (WSNs) are envisioned to be a widely utilized technology in Smart Grid (SG). Maximizing Network Lifetime (NL) of WSNs in SG deployments is necessary to provide reliability and efficiency of the services offered to the entities involved. Harsh channel conditions in SG environments have a profound impact on the communication channel utilized by WSNs. Therefore, optimizing the Transmission Power Level (TPL) and Data Packet Size (DPS) is of paramount importance for prolonging WSN NL. In both TPL and DPS optimizations two general approaches are followed: utilizing a constant TPL and/or DPS or optimizing TPL and/or DPS for each link. However, joint optimization of TPL and DPS for each link has not been investigated in the literature. In this study we present a Mixed Integer Programming (MIP) framework which utilizes a detailed link layer abstraction to analyze nine TPL and DPS assignment strategies for WSNs employed in SG environments. The results of our analysis reveal that there is a large margin to be exploited in prolonging WSN NL by appropriate selection of the strategy to be used in TPL and DPS optimization.**

***Index Terms*—Wireless sensor networks, packet size optimization, transmission power control, mixed integer programming, smart grid, network lifetime.**

I. Introduction

SMART Grid (SG) is envisioned to be a cyber-physical energy and information Internet with tight coupling of its ICT (Information & Communication Technologies) and power system constituents [1]. Enabling effective information flow within the framework of SG is necessary for the efficient operation of the whole system. Since SG encompasses various domains with different information flow requirements, utilization of multiple communication technologies in SG is inevitable [2], [3]. Among these communication technologies, Wireless Sensor Networks (WSNs) are recognized as a promising technology for various SG application areas. Monitoring power equipment, power lines, and other components of the power system through WSNs will enable the early diagnosis of possible problems (due to natural or man made hazards and equipment malfunctions) which will alert the system operators to take remedial action in a timely manner, hence, contributing to the efficiency, reliability, and safety of SG. Moreover, data gathered by WSNs will be invaluable in efficient demand response control, decision making for dynamic pricing, renewable energy output forecasting, demand prediction, and surveillance of the premises [4], [5].

H. U. Yildiz is with the Department of Electrical and Electronics Engineering, TED University, 06420, Ankara, Turkey (e-mail: hugur.yildiz@tedu.edu.tr)

S. Kurt and B. Tavli are with the Department of Electrical and Electronics Engineering, TOBB University of Economics and Technology, 06560, Ankara, Turkey (e-mail: skurt@etu.edu.tr, btavli@etu.edu.tr).

WSNs, in general, and WSNs utilized in SG applications, in particular, are required to operate for prolonged periods of time which dictates that all aspects of WSNs should be designed to provide energy efficiency and to maximize Network Lifetime (NL) [5]. In a typical WSN scenario, most of the energy dissipated in sensor nodes are due to the communication operations, hence, it is especially important to eliminate sources of energy waste in communication related tasks [1]. Optimizing sensor nodes' sleep/awake cycle, elimination of redundant data transmissions, minimizing energy waste on packet collisions, Transmission Power Control (TPC), and Data Packet Size (DPS) optimization are the techniques (among others) utilized for NL maximization [6]. One of the challenges for WSNs deployments in SG environments is the harsh communication channel conditions, hence, optimization of TPL and DPS is particularly important.

On a certain link if the utilized power level is too low than most of the transmitted packets will contain bit errors which necessitates the repetition of the costly handshake. On the other hand, utilizing a power level much higher than the optimal power level will lead to energy waste without any significant performance improvements [7]. Utilizing a low DPS is preferable for minimizing the Packet Error Rate (PER), in general, however, the ratio of payload to overhead (*i.e.*, data packet header/trailer and Acknowledgement – ACK – packets) bits is also lower for shorter packets. Longer data packets have the advantage of higher payload to overhead ratio which leads to better energy efficiency, yet, PER for longer packets are also high, in general. Furthermore, TPL and DPS decisions are interrelated affecting the choice of one another, hence, joint optimization of these two parameters are necessary for maximizing WSN NL. Moreover, whether the optimization of TPL and DPS is done locally or globally is of practical interest (*i.e.*, should the optimization decisions be made network-level or link-level?).

The literature on TPC and DPS optimization for WSNs is rich [6], [8]–[22]. TPC in WSNs is done by using two distinct approaches: network-level TPC [10], [11] and link-level TPC [12]–[16]. On all links in the network the same power level (*e.g.*, maximum level) is utilized in network-level TPC approaches. In link-level TPC approaches, TPL on each link can be different. Likewise, DPS optimization can be done by using a single DPS for the whole network [17], [18] or by optimizing DPS for each link [19]–[21]. Joint optimization of TPL and DPS is investigated in [6], [22], however, in these studies DPS optimization is done by utilizing a single DPS for all the links. We will present a detailed literature overview on TPC and DPS optimization in Section II.

The contributions of this study are threefold:

1) In WSN literature, NL maximization through joint optimization of TPL and DPS for each link has never been investigated. Therefore, to fill the gap in the literature, we created a novel strategy that jointly optimizes both TPL and DPS for each link to maximize NL.
2) The performance gains brought by our novel strategy can only be revealed when it is quantitatively compared against other TPL and/or DPS assignment approaches reported in the literature. Therefore, we created a novel family of Mixed Integer Programming (MIP) models to be able to analyze eight strategies (in addition to the novel strategy we created) under ideal, yet, practical and fair conditions. Most of our strategies are inspired by the studies in the literature [6], [10]–[13], [15], [17]–[28].
3) Through the numerical evaluations of the nine TPL and DPS assignment strategies, we characterized the performance bounds of these strategies quantitatively. We employed a detailed link-layer abstraction which is based on Tmote Sky motes' characteristics. We also utilized experimentally verified path loss models with six different parameter sets for Tmote Sky motes in SG environments.

The rest of the paper is organized into five sections. Related work is presented in Section II. We present the MIP models of the nine strategies in Section III. The link-layer abstraction and the energy model is elaborated in Section IV. Comparative analysis of the strategies are given in Section V. Conclusions and future research directions are given in Section VI.

II. Related Work

One of the main objectives of this study is to present a comparative evaluation of the TPL and DPS optimization techniques. We introduce nine strategies in Section III most of which are inspired by the existing studies in the literature. In this section, we will elaborate on the studies in literature which are abstracted in our strategies (*i.e.*, we will establish the relationships between our strategies and the literature) in the subsequent subsections.

A. Variable Packet Size and Variable Transmission Power

VPVT (Variable Packet size and Variable Transmission power) and VPVT-L (VPVT through Local optimization) strategies are novel strategies which have never been investigated in the context of WSN NL maximization. However, VPVT-L strategy was investigated in the context of cooperative communications in [18]. Indeed, a three-node configuration consisting of a sender, a receiver, and a relay is investigated through an optimization formulation (*i.e.*, only a single cooperative link is considered).

B. Variable Packet Size and Constant Transmission Power

VPCT (Variable Packet size and Constant Transmission power) strategy is inspired by [21] where a framework for DPS optimization is formulated in the context of cognitive radio sensor networks. However, transmission power optimization is not performed in this study. VPCT-L (VPCT through Local optimization) strategy is employed in [19], [20]. In [19], a distributed scheme (Dynamic Packet Length Control – DPLC) is presented which optimizes the packet length for each link. In [20], DPS optimization for energy efficiency in delay-tolerant sensor networks is investigated through an analytical framework. Nevertheless, TPC is not addressed in [19], [20].

C. Constant Packet Size and Variable Transmission Power

CPVT (Constant Packet size and Variable Transmission power) strategy is investigated in [11], [12], [23], [29], [30]. In [11], various TPC strategies with fixed DPS assumption is investigated via an optimization model in WSNs. In [12], a TPC approach to achieve a predefined Packet Delivery Ratio (PDR) at each link is proposed. In [23], TPC in multi-channel WSNs is investigated through an optimization framework. Constant DPS are utilized in both [12], [23]. In [29], [30], TPC optimization frameworks considering the interference created by the nodes themselves for social-aware and social-oriented wireless networks are presented.

CPVT-L (CPVT through Local optimization) strategy is perhaps the most frequently utilized strategy in the literature [6], [10], [13], [15], [17], [22], [24], [25]. The common features of these studies are utilization of fixed DPSs and link-level TPL optimization. In [6], [22], joint optimization of TPL and DPS are investigated. Although, in both studies, TPC is link-level (*i.e.*, optimal TPL for each link is assigned), DPS optimizations are network-level (*i.e.*, a single optimal DPS for the whole network is utilized). In [10], various link-level and network-level TPC strategies for WSN NL maximization are investigated by using an optimization framework. In [13], probe based path loss estimation and transmission power optimization are investigated to improve network dependability in WSNs. In [15], a lightweight TPC algorithm for WSNs (Adaptive TPC – ATPC) is presented. In [24], experimental evaluations of various WSN TPC techniques are performed by using a large WSN testbed. In [25], optimal transmission power policies for WSNs equipped with solar panels are investigated. In [17], effects of various physical layer parameters including TPL on energy efficiency of WSNs are investigated through mathematical analysis and simulations.

D. Constant Packet Size and Constant Transmission Power

CPCT (Constant Packet size and Constant Transmission power) strategy is utilized in [26]–[28]. In fact, common features of these studies are utilization of a constant TPL and constant DPS throughout the network in terrestrial [26], [27] and underwater [28] WSNs. Note that unlike CPCT strategy, there is no network-level optimization of transmission power or DPS in these studies. However, for the sake of a fair comparison we utilize optimized power levels and DPSs as opposed to arbitrary transmission power and DPS utilization.

E. Maximum Transmission Power

MxPMxT (Maximum Packet size and Maximum Transmission power) and MnPMxT (Minimum Packet size and Maximum Transmission power) strategies are utilized for benchmarking the performance gains brought by other strategies.

For example, the maximum TPL and constant DPS strategy is used to benchmark the other strategies in [11], [12].

Most of our strategies are inspired by the studies in the literature. However, we utilize only the main design philosophies of these studies in our strategies. In this study, all our strategies are evaluated under exactly the same assumptions and scenarios, hence, one of our novel contributions to the literature is by providing quantitative and fair comparisons of a large set of TPL and DPS optimization strategies for WSN NL maximization.

III. Optimization Framework

NL maximization problem is constructed by considering the network as a directed graph where nodes are represented by the set V and node-1 is chosen as the base station. The set W is defined such that node-1 is excluded from the sensor nodes (*i.e.*, $W = V \setminus \{1\}$). The set of arcs is defined as $A = \{(i,j) : i \in W, j \in V - i\}$. Throughout this work, the amount of data flowing (*i.e.*, number of data packets) from node-i to node-j is represented as f_{ij} (possibly by adding various superscripts). Variable or constant DPSs are expressed by η (with various indices).

We create nine MIP models for DPS and TPL assignment as representative strategies which are presented in the subsequent subsections. For all strategies data flows on the links are optimized to maximize NL which facilitates a fair comparison of all strategies by utilizing an idealized routing layer. We first present four basic strategies which differentiate in the way that DPS and transmission power optimization are done.

A. Variable Packet size and Variable Transmission power (VPVT) Strategy

The optimization framework constructed in this subsection maximizes NL by globally optimizing power levels for data/ACK packets, and DPSs utilized on each link. The objective function of this problem is to maximize NL in terms of rounds (N_{rnd}) expressed as

$$\text{Maximize } N_{rnd}. \tag{1}$$

Round duration is denoted by $T_{rnd} = 20$ s. Constraints of the optimization problem are given in Eqs. (2) to (7).

$$N_{rnd} \times s_i + \sum_{l,k \in S_L} \sum_{m \in S_M} \sum_{(j,i) \in A} \eta^m f_{ji}^{lkm} = \sum_{l,k \in S_L} \sum_{m \in S_M} \sum_{(i,j) \in A} \eta^m f_{ij}^{lkm}, \ \forall i \in W. \tag{2}$$

Constraint in Eq. (2) is used to model the flow balancing at each sensor node ($\forall i \in W$). In this constraint, $s_i = 120$ Bytes is the generated data in every node at each round and η^m is the payload size in terms of Bytes. Note that values of η^m are calculated by using the $\eta^m = 120/m$ relation (*e.g.*, for $m = 4$, $\eta^4 = 120/4 = 30$ Bytes) with $m \in S_M = \{1,2,3,4,5,6\}$. Decision variables, f_{ji}^{lkm}, represent the number of incoming packets from node-j to node-i, transmitted at power level-l and acknowledged (ACK) at level-k with the payload length of η^m. This constraint simply states that the sum of incoming flows and data generated in each sensor node is equal to sum of outgoing flows (in Bytes).

Each node is busy as long as data acquisition or transmission/reception occurs. The total busy time of a sensor node can be calculated as

$$T_{bsy,i} = N_{rnd} \times T_{DA} + \sum_{l,k \in S_L} \sum_{m \in S_M} T_{slot}^m \times \left[\sum_{(i,j) \in A} \lambda_{ij}^{lkm} f_{ij}^{lkm} + \sum_{(j,i) \in A} \lambda_{ji}^{lkm} f_{ji}^{lkm} \right], \forall i \in W, \tag{3}$$

where T_{slot}^m is the slot time dedicated for data transmission/reception at each node which is a function of DPS. λ_{ij}^{lkm} is the average number of retransmissions to account for handshake failures and T_{DA} is the data acquisition time for sensor nodes to gather information from the environment. If a node is not busy then it is in the sleep state. The energy balancing constraint given in Eq. (4) states that the sum of transmission/reception, acquisition, and sleep energies is limited by the battery of each sensor node

$$\sum_{l,k \in S_L} \sum_{m \in S_M} \left[\sum_{(i,j) \in A} E_{tx,ij}^{lkm} f_{ij}^{lkm} + \sum_{(j,i) \in A} E_{rx,ji}^{lkm} f_{ji}^{lkm} \right] + P_{slp}(N_{rnd} T_{rnd} - T_{bsy,i}) + N_{rnd} E_{DA} \leq \epsilon_i, \forall i \in W. \tag{4}$$

In the energy balancing constraint, $E_{tx,ij}^{lkm}$ and $E_{rx,ji}^{lkm}$ are energy consumptions in transmit and receive states (including retransmissions). P_{slp} is the power consumption in sleep state and E_{DA} is the data acquisition energy. The overall energy consumption for each node is limited by the initial node energy, $\epsilon_i = 4$ KJ.

The constraint given in Eq. (5) models the total bandwidth usage in the network which states that overall outgoing, incoming, and interfering flows are bounded by total NL.

$$\sum_{l,k \in S_L} \sum_{m \in S_M} \left[\sum_{(i,j) \in A} \lambda_{ij}^{lkm} f_{ij}^{lkm} + \sum_{(j,i) \in A} \lambda_{ji}^{lkm} f_{ji}^{lkm} + \sum_{(j,n) \in A} \lambda_{jn}^{lkm} f_{jn}^{lkm} I_{jnlk}^i \right] T_{slot}^m \leq N_{rnd} T_{rnd}, \ \forall i \in V. \tag{5}$$

Constraints stated in Eqs. (5) and (6) are derived from the condition given in [10]. Interference occurs at node-i due to data transfer between node-j and node-n (or ACK transfer in the reverse path). It is unity either when node-j transmits data to node-n at power level-l or when node-n sends ACK to node-j at power level-k and received power at node-i is greater than the sensitivity level.

$$I_{jn}^i(l,k) = \begin{cases} 1, \text{ if } P_{rx,ji}^{in,l} \geq P_{sns} \text{ or } \\ \quad P_{rx,ni}^{in,k} \geq P_{sns} \ . \\ 0, \text{ o.w.} \end{cases} \tag{6}$$

In the above equation, P_{sns} is the sensitivity level, $P_{rx,ji}^{in,l}$ and $P_{rx,ni}^{in,k}$ denote the input powers of node-i's receiver due to the transmission from node-j and node-n. The constraint

given in Eq. (7) states the non-negativity criteria of the data flows as

$$f_{ij}^{lkm} \geq 0,\ \forall (i,j) \in A, \forall l \in S_L, \forall k \in S_L, \forall m \in S_M. \quad (7)$$

The MIP model described by Eqs. (1)–(7) is, actually, the base model we utilize to build the other eight MIP models presented in the subsequent subsections.

B. Variable Packet size and Constant Transmission power (VPCT) Strategy

In VPCT strategy only DPSs are allowed to take the optimal values for each link whereas the data/ACK TPLs are constant throughout the network. The optimal constant data/ACK TPLs are determined by adding the following constraints to the MIP model given in Section III-A as

$$\sum_{m \in S_M} \sum_{(i,j) \in A} f_{ij}^{lkm} \leq M \times a_{lk}, \forall l \in S_L, \forall k \in S_L, \quad (8)$$

$$\sum_{(l,k) \in S_L} a_{lk} \leq 1. \quad (9)$$

Eq. (8) is used to assign values to the binary variables a_{lk} (*i.e.*, $a_{lk} = 1$ if there is any flow in the network using data/ACK TPLs of l and k, otherwise $a_{lk} = 0$). We use a large integer (M) to convert the integer values to the binary indicator variable (*i.e.*, the big M technique is a well-known and widely utilized technique in MIP formulations). Eq. (9) makes sure that there can be only one pair of (l,k) for the entire network which are the optimal data/ACK TPLs.

C. Constant Packet size and Variable Transmission power (CPVT) Strategy

In CPVT strategy, TPLs are optimized for each link, however, the DPS is constant throughout the network. The following constraints are used in addition to the model presented in Section III-A to model the CPVT strategy

$$\sum_{(l,k) \in S_L} \sum_{(i,j) \in A} f_{ij}^{lkm} \leq M \times a_m, \forall m \in S_M, \quad (10)$$

$$\sum_{m \in S_M} a_m \leq 1. \quad (11)$$

Eq. (10) is used to assign values to the binary indicator variables a_m and Eq. (11) guarantees that only one DPS is utilized throughout the network.

D. Constant Packet size and Constant Transmission power (CPCT) Strategy

In CPCT strategy, TPLs and DPSs are constant throughout the network (*i.e.*, all nodes use the same DPS and the same data/ACK TPLs). By inserting the following constraints to the VPVT model, we obtain the CPCT model as

$$\sum_{(i,j) \in A} f_{ij}^{lkm} \leq M \times a_{mlk}, \forall m \in S_M, \forall l \in S_L, \forall k \in S_L, \quad (12)$$

$$\sum_{(l,k) \in S_L} \sum_{m \in S_M} a_{mlk} \leq 1. \quad (13)$$

Eq. (12) is used to assign values to the binary indicator variables a_{mlk} and Eq. (13) guarantees that only one DPS and only one pair of (l,k) is utilized throughout the network (*i.e.*, the optimal network-level DPS and data/ACK TPLs).

The four strategies presented so far are based on global optimization of TPLs and DPS. However, in practice local optimizations are preferable (*i.e.*, the assignment of TPLs and DPSs are link-scope decisions as opposed to network-scope decisions). Therefore, in the following subsections we present three strategies using local optimizations of power level and/or DPS.

E. Variable Packet size and Variable Transmission power through Local optimization (VPVT-L) Strategy

In VPVT-L strategy, data/ACK TPLs and DPSs are determined through link-scope optimization. The main idea in this strategy is to jointly determine local optimal power levels as well as optimal DPS on each (i,j) link, which can be formulated as

$$\{l_{ij}, k_{ji}, m_{ij}\} = \underset{l,k,m}{\operatorname{argmin}} \left(\frac{E_{tx,ij}^{lkm} + E_{rx,ji}^{lkm}}{\eta^m} \right), \forall (i,j) \in A. \quad (14)$$

Total energy dissipation for the same amount of data transfer is minimized by utilizing Eq. (14). After determining the optimal power levels (*i.e.*, $\{l_{ij}, k_{ji}\}$) and DPS (*i.e.*, m_{ij}) on each link, we modify the flow decision variables for the MIP model presented in Section III-A with f_{ij} by dropping l, k, and m superscripts from notations. Note that, we remove $\sum_{(l,k) \in S_L}$ and $\sum_{m \in S_M}$ summations in the constraints of the VPVT model.

F. Variable Packet size and Constant Transmission power through Local optimization (VPCT-L) Strategy

The difference between VPCT and VPCT-L strategies is that in VPCT-L strategy DPS optimizations on each link are done locally. Local optimization is achieved by determining the DPS for each link that minimizes the energy dissipation for transmission and reception which is formulated as

$$\{m_{ij}^{lk}\} = \underset{m}{\operatorname{argmin}} \left(\frac{E_{tx,ij}^{lkm} + E_{rx,ji}^{lkm}}{\eta^m} \right), \forall (i,j) \in A, \forall l,k \in S_L. \quad (15)$$

After determining the optimal DPSs on each link locally, we modify the flow decision variables with f_{ij}^{lk} by dropping m superscripts from notations. We also remove $\sum_{m \in S_M}$ summations in the constraints of the VPCT optimization model.

G. Constant Packet size and Variable Transmission power through Local optimization (CPVT-L) Strategy

In CPVT-L strategy TPL assignments are done locally on all links by using the following local optimization formulation

$$\{l_{ij}^m, k_{ji}^m\} = \underset{l,k}{\operatorname{argmin}} \left(\frac{E_{tx,ij}^{lkm} + E_{rx,ji}^{lkm}}{\eta^m} \right), \quad \forall (i,j) \in A, \forall m \in S_M. \quad (16)$$

When determining data/ACK TPLs on each link, we modify the flow decision variables with f_{ij}^{m} by dropping the (l,k) superscripts from notations. We also remove $\sum_{(l,k)\in S_L}$ summations in the constraints of the CPVT optimization model.

Note that, we have only three local optimization strategies as opposed to the four global optimization strategies due to the definition of CPCT strategy which does not have a localized version. To facilitate a benchmark for the comparison, we design two more strategies which do not utilize any DPS and/or TPL optimization mechanisms and they are presented in the following two subsections.

H. Maximum Packet size and Maximum Transmission power (MxPMxT) Strategy

For practical applications that aim to minimize the packet loss, the maximum available TPL can be used throughout the network without optimizing TPLs. Utilizing the maximum possible power level as the predetermined data and ACK packet TPLs (*i.e.*, l_{max}) reduces the complexity of the optimization problem and it increases the successful data reception rate at the cost of excess energy consumption. In the MxPMxT strategy data/ACK TPLs as well as DPSs take the maximum values available. Implementation of this model is straightforward. We modify the flow decision variables in VPVT model with f_{ij} by dropping the (l,k,m) superscripts (*i.e.*, flow optimization is still done globally). We also remove $\sum_{(l,k)\in S_L}$ and $\sum_{m\in S_M}$ summations in the constraints of the VPVT optimization model.

I. Minimum Packet size and Maximum Transmission power (MnPMxT) Strategy

Utilizing the minimum DPS is more advantageous than using the maximum DPS in networks composed of low Signal-to-Noise Ratio (SNR) links. Therefore MnPMxT strategy has a potential to result in higher NLs than MxPMxT strategy for harsh channels. The implementation of the MnPMxT strategy is similar to MxPMxT except that DPS utilized is the minimum DPS available. Note that, we do not create a minimum power strategy because if we force all links to use minimum power levels then network disconnection becomes frequent which prevents us from performing analysis especially in sparser network configurations.

IV. Energy Dissipation Model

In this section we present our energy dissipation model and its parameters (*i.e.*, $E_{tx,ij}^{lkm}$ and $E_{rx,ji}^{lkm}$) which are used in energy balancing constraint (*i.e.*, Eq. (4)), presented in the optimization framework outlined in Section III. These parameters are specific for the sensor node platform used in the network (*i.e.*, Tmote Sky motes). Experimentally obtained Tmote Sky platform characteristics (equipped with a Chipcon CC2420 radio as the communication unit and a TI MSP430 microcontroller as the control unit [31]) are utilized in our framework.

At the data link layer, a dynamic Time Division Multiple Access (TDMA) Medium Access Control (MAC) layer is assumed to be in operation [32]. Each node communicates in its dedicated slot and is in the sleep mode when it is neither in communication nor in data acquisition states. In each round, every node dissipates a certain amount of data acquisition energy, E_{DA}, that can be calculated by multiplying acquisition power, P_{DA}, with acquisition time, T_{DA}. In the data acquisition phase, microcontroller and sensor boards are active (*i.e.*, P_{DA} = 5.4 + 6 = 11.4 mW) for T_{DA} = 5 ms duration, therefore E_{DA} is equal to 57 μJ. Energy dissipation in other states are dependent on the durations of the states. For example, the sleep power consumption, P_{sleep} is given as 3 μW. Receive power consumption is P_{rx} is 69 mW and transmit power consumption is denoted as P_{tx} which depends on the output power level-l. $P_{tx}^{out,l}$ is the output antenna power for Chipcon CC2420 transceivers (in dBm) and documented power consumptions and corresponding output power levels for the Tmote sky platform are presented in Table I [31].

We employ a log-normal shadowing model as given in Eq. (19) and the parameters of the model are given in Table II, which are obtained by direct experimentation and curve fitting of the experimental data. However, we do not utilize a fading model because in the networks we consider all nodes are static (*i.e.*, there is no relative motion between the transmitter and receiver nodes). Even if the transmitter-receiver pairs are static the channel between them can change in time, yet, we believe such dynamic variations are not frequent and too fast in our scenarios. Hence, we assume that temporal variations are mainly due to fluctuations in the thermal noise of the radios in our model [33].

Reliable communication between nodes is achieved via handshaking (*i.e.*, successful data packet reception is acknowledged with ACK packets). To calculate the Packet Error Rate (PER), bit error rate (BER) is needed and it can be calculated by using the SNR, χ_{ij}^{l} (in dB), which is formulated as

$$\chi_{ij}^{l} = P_{rx,ij}^{in,l} - P_n, \tag{17}$$

where $P_{rx,ij}^{in,l}$ denotes the input power at the receiver-j for the data packet transmitted at power level-l from node-i to node-j. P_n is the total noise power on the effective receiver bandwidth including noise figure of the receiver. $P_{rx,ij}^{in,l}$ can be calculated as

$$P_{rx,ij}^{in,l} = P_{tx}^{out,l} - \phi_{ij}, \tag{18}$$

where $P_{tx}^{out,l}$ is the output power level in dBm at power level-l. ϕ_{ij} is the path loss on (i,j) link which is calculated with the log-normal shadowing model (in dB) as

$$\phi_{ij} = \phi_0 + 10n\log_{10}\left(\frac{d_{ij}}{d_0}\right) + X_\sigma, \tag{19}$$

where ϕ_0 is the reference path loss at the reference distance d_0, d_{ij} is the distance between node-i and node-j, n is the path loss exponent, and X_σ is a Gaussian random variable with zero mean and standard deviation σ (in dB). Path loss parameters for the six SG environments which are adopted in this work are presented in Table II [5].

Using the SNR value obtained with Eqs. (17)–(19) and adding Processing Gain (G_P) which is 8 ($\frac{2Mchip/s}{250Kbit/s}$) for Tmote

TABLE I: Transmission power levels (l), antenna output powers $P_{tx}^{out,l}$ (in dBm), and circuit power consumptions P_{tx}^{l} (in mW) for Tmote Sky motes.

l	P_{tx}^{l}	$P_{tx}^{out,l}$	l	P_{tx}^{l}	$P_{tx}^{out,l}$
1	25.5	-25	5	41.7	-5
2	29.7	-15	6	45.6	-3
3	33.6	-10	7	49.5	-1
4	37.5	-7	8 (l_{max})	52.2	0

TABLE II: Path Loss Exponent (n), Standard Deviation (σ – dB), and Total Noise Power (P_n – dBm) for six SG environments.

Environment	n	σ	P_n
Outdoor 500 KV Substation-LOS, (OutLOS)	2.42	3.12	-93
Outdoor 500 KV Substation-NLOS, (OutNLOS)	3.51	2.95	-93
Indoor Main Power Room-LOS, (InLOS)	1.64	3.29	-88
Indoor Main Power Room-NLOS, (InNLOS)	2.38	2.25	-88
Underground Network Transformer Vault-LOS, (UndLOS)	1.45	2.45	-92
Underground Network Transformer Vault-NLOS, (UndNLOS)	3.15	3.19	-92

Sky, BER (ρ_e) for Offset Quadrature Phase Shift Keying (O-QPSK) is calculated as

$$\rho_e = Q\left(\sqrt{\frac{2E_b}{N_0}}\right), \tag{20}$$

where $\frac{E_b}{N_0} = \chi_{ij}^{l} G_P$. Once ρ_e is obtained, the probability of receiving an η Bytes packet without error is obtained as

$$\rho_{ij}^{l,s}(\eta) = \left(1 - Q\left(\sqrt{16\chi_{ij}^{l}}\right)\right)^{8\eta}. \tag{21}$$

Hence PER, $\rho_{ij}^{l,f}(\eta)$, is

$$\rho_{ij}^{l,f}(\eta) = 1 - \rho_{ij}^{l,s}(\eta). \tag{22}$$

The two-way successful handshake probability ($\beta_{ij}^{lkm,s}$) for η^m Bytes data packet transmitted at power level-l and an η^a Bytes ACK packet transmitted at power level-k can be calculated as

$$\beta_{ij}^{lkm,s} = \rho_{ij}^{l,s}(\eta^m) \times \rho_{ji}^{k,s}(\eta^a). \tag{23}$$

Therefore, the failed handshake probability is $1 - \beta_{ij}^{lk,s}$.

Retransmissions should be considered to account for the failed handshaking case. On the average, packet retransmission rate is $\lambda_{ij}^{lkm} = \frac{1}{\beta_{ij}^{lkm,s}}$.

By denoting $T_{tx}(\eta^m)$ as the duration to transmit η^m Bytes of data, the energy dissipation value for transmitting an η^m Bytes packet is given as

$$E_{tx}^{l}(\eta^m) = P_{tx}^{l} T_{tx}(\eta^m). \tag{24}$$

In an active slot after transmitting the data packet, a node will be in the reception mode for a duration of $T_{slot}^{m} - T_{tx}(\eta^m)$, hence, the total energy dissipation of data transmitting node in a two-way handshake is,

$$E_{tx}^{HS,ls}(\eta^m) = E_{tx}^{l}(\eta^m) + P_{rx}(T_{slot}^{m} - T_{tx}(\eta^m)). \tag{25}$$

The average transmission energy dissipation increases due to the retransmissions which can be modeled as

$$E_{tx,ij}^{lkm} = E_P^m + \lambda_{ij}^{lkm} E_{tx}^{HS,l}(\eta^m), \tag{26}$$

where E_P^m is the packet processing energy which varies with the DPS and is equal to utilization time of processor times the active mode power consumption value of the nodes (12.66 μJ for a 120 Bytes of payload). On the other hand, the energy dissipation of the node that is receiving data and responding with an ACK packet at TPL-k is

$$E_{rx}^{HS,ks}(\eta^a) = E_{tx}^{k}(\eta^a) + P_{rx}(T_{slot}^{m} - T_{tx}(\eta^a)). \tag{27}$$

This energy does not change for the case of handshake failure due to ACK packet failure. However, if the handshake failure is due to data packet failure then the energy dissipation of the receiver node changes as

$$E_{rx}^{HS,f} = P_{rx} T_{slot}^{m}. \tag{28}$$

Including retransmissions average energy dissipation of the receiver node becomes

$$\begin{aligned} E_{rx,ji}^{lkm} = E_P^m + \lambda_{ij}^{lkm} \Big[\beta_{ij}^{lkm,s} E_{rx}^{HS,k}(\eta^a) + \\ \rho_{ij}^{l,s}(\eta^m) \rho_{ji}^{k,f}(\eta^a) E_{rx}^{HS,ks}(\eta^a) + \rho_{ij}^{l,f}(\eta^m) E_{rx}^{HS,f} \Big]. \end{aligned} \tag{29}$$

For the slot time calculation, the propagation delay is chosen as $T_{prop} = 100$ μs and guard times are used to prevent synchronization errors [11]. The guard time is chosen as $T_{grd} = 100$ μs that is larger than twice the worst case synchronization error that can be achieved by available synchronization protocols [6]. For η^m Bytes of data payload and $\eta^h = 8$ Bytes of header, the total DPS (η^P) is equal to $\eta^m + \eta^h$. Also $\eta^a = 12$ Bytes is the ACK packet size. Therefore the variable slot time is calculated as

$$T_{slot}^{m} = 2 \times T_{grd} + T_{tx}(\eta^P) + T_{prop} + T_{tx}(\eta^a), \tag{30}$$

where $T_{tx}(\eta^P)$ and $T_{tx}(\eta^a)$ are the durations to transmit data and ACK packets, respectively. These values are equal to the total number of bits transmitted divided by data rate in the wireless channel (250 Kbps). For example, for a 128 Bytes data packet (*i.e.*, $\eta^P = 128$ Bytes) the slot time is 4.78 ms.

V. Analysis

In this section, we explore the performance of DPS and TPL assignment strategies for SG WSN applications from NL perspective by utilizing the numerical evaluations of the MIP models. We use MATLAB to construct the instances of the physical layer model parameters presented in Section IV. General Algebraic Modeling System (GAMS) is employed for the solutions of the MIP framework presented in Section III. GAMS consists of high-performance solvers for solving MIP models to optimality and we opted to utilize the CPLEX solver which employs algorithms such as branch-and-bound, branch-and-cut, etc. Nevertheless, specific implementation details are beyond the scope of this study. We first present the analysis of a line network with five nodes (*i.e.*, toy example) to reveal the characteristics of our four main strategies (*i.e.*, VPVT, VPCT, CPVT, and CPCT) and two benchmark strategies

(*i.e.*, MxPMxT and MnPMxT) in Section V-A. The main purpose of providing such a toy example is two-fold. First, the toy example serves as a visual description of our strategies. Second, comprehension of our larger scale analysis presented in Section V-B is enhanced by using such a pedagogical introductory analysis.

A. Toy Example

In this subsection, we present our analysis on a small scale topology in Fig. 1. The toy example is constructed as a linear topology which consists of five nodes where the distance between adjacent nodes (*i.e.*, d_{int}) is 35 meters and node-1 is the base station with the coordinates (0,0). Path losses between nodes are determined randomly according to Eq. (19). The SG environment is chosen as OUS-L. In each sub-figure, we show data flows for different strategies. NL is normalized in a way that NL obtained with VPVT strategy is 1000 rounds. NLs obtained with VPCT, CPVT, CPCT, MxPMxT, and MnPMxT strategies are 990, 950, 940, 740, and 750 rounds, respectively (*e.g.*, CPVT NL is 5.0% lower than VPVT NL).

The flow variables are denoted as f_{ij}^{lkm}, f_{ij}^{m}, and f_{ij}^{lk} for VPVT, VPCT, and CPVT strategies, respectively. Note that in these definitions, index m shows the payload size, l and k are the data and ACK TPLs, respectively. Since all nodes use the same DPS and same data/ACK TPLs in CPCT strategy (for a particular topology) and for MxPMxT/MnPMxT strategies (for all topologies) we use f_{ij} to represent the flows for these strategies.

In Fig. 1a, data flows for the VPVT strategy are presented. 1000 data packets with 120 Bytes of payload (*i.e.*, $m = 1$) are transmitted from node-5 to node-4 (*i.e.*, $i = 5$ and $j = 4$) by using the highest TPLs for both data and ACK packets (*i.e.*, $l = k = 8$). Node-4 transmits its own generated data plus node-5's data to node-3 by using power levels 7 and 5 for data and ACK packets, respectively, by using the payload size of 120 Bytes. Node-3 splits its data into two parts where 2994 packets of 120 Bytes payload (*i.e.*, $m = 1$) are transmitted to node-2 and 36 packets of 20 Bytes payload (*i.e.*, $m = 6$) are transmitted to node-1. Note that total incoming data to node-3 is 2000 packets $\times$ 120 Bytes = 240 KB. The amount of data generated at node-3 is 1000 rounds $\times$ 120 Bytes = 120 KB. The total amount of data flowing out of node-3 is 2994 packets $\times$ 120 Bytes + 36 packets $\times$ 20 Bytes = 360 KB. Although the length of link-(4,3) and link-(2,1) are the same, path loss value on link-(4,3) is higher than the path loss value on link-(2,1) due to shadowing term in Eq. (19). To mitigate the effects of higher path loss node-2 transmits its data with higher TPLs and lower DPS in comparison to node-4 (*i.e.*, f_{43}^{751} versus f_{21}^{883}).

For this toy example, the maximum TPL is utilized for both data and ACK packets in VPCT strategy. For CPVT strategy, the optimum DPS is determined as 60 Bytes. For CPCT strategy, the maximum TPL is utilized (for both data and ACK packets) throughout the network and the optimum DPS is 60 Bytes. Nevertheless, our analysis on single small scale network is not sufficient to characterize our strategies, therefore, we extend our analysis on large scale networks in the following subsection.

B. Disk Topology

We perform the numerical evaluations on a disk shaped topology with radius R_{net}. We utilized three different network radii for each SG environment and 50 sensor nodes are uniformly distributed within the disk. For statistical significance, 100 randomly generated topologies are used. The base station is located at the center of the network. Moreover, we investigate the impact of channel conditions on NL by considering six different SG environments (see Table II). In total we solve 16200 different optimization problems (*i.e.*, 9 strategies, 6 environments, 3 network radii, and 100 randomly generated topologies) for the detailed analysis.

We present the results of our numerical analysis in Figs. 2–5. In Fig. 2, we present average NL values for all nine strategies in six SG environments. For each environment, we utilized three network radii to assess the impact of node density on NL. The largest network radius in each topology is chosen in such a way that disconnected network topologies due to the extended inter-node distances are not more than 10% of all generated random topologies. Nevertheless, R_{net} values are chosen in such a way that average successful handshake probabilities, given in Eq. (23), for the lowest, the medium, and the largest radii in each scenario are, approximately, 0.99, 0.50, and 0.10, respectively. Average DPSs, data, and ACK TPLs for all strategies are given (*i.e.*, for MnPMxT and MxPMxT strategies DPSs and TPLs are all predetermined and fixed) in Figs. 3–5, respectively.

Chosen R_{net} values vary for each SG environment because the average path loss values differ significantly. For example $R_{net} > 40$ m results in highly disconnected topologies for OutNLOS, whereas, for InLOS environment $R_{net} \leq 100$ m, all network topologies are strongly connected. The harshness of the channel is a combined effect of the n, σ, and P_n parameters for each environment. Hence, the path loss in SG environments can be assorted from the harshest to the mildest (for a given link distance) as follows: OutNLOS, UndNLOS, InNLOS, OutLOS, InLOS, and UndLOS. All three NLOS environments have the higher path loss values in comparison to the three LOS environments. In fact, average communication ranges are higher in milder SG propagation environments.

For all strategies, NLs decrease as R_{net} increases. Because increasing R_{net}, simply, means that sensor nodes either need to set higher TPLs or to use smaller DPSs. Both options result in more energy consumption, consequently decreasing NL.

In all SG environments and for all node densities, VPVT strategy gives the highest NLs. In fact, VPVT has the highest degree of freedom in assigning DPSs and TPLs among all strategies which is the reason for its superior performance in comparison to other strategies. Therefore, we will use VPVT as our gold standard in this study to benchmark all other strategies (*i.e.*, VPVT defines the upper limit of what can be achieved in our framework). VPVT utilizes the higher DPSs (*e.g.*, average DPSs for VPVT are in close vicinity of 120 Bytes) in all densest networks because in dense networks most of the links have path loss values that can be compensated by employing high enough TPLs to ensure low PER, thus, utilizing the highest DPS is the most favorable

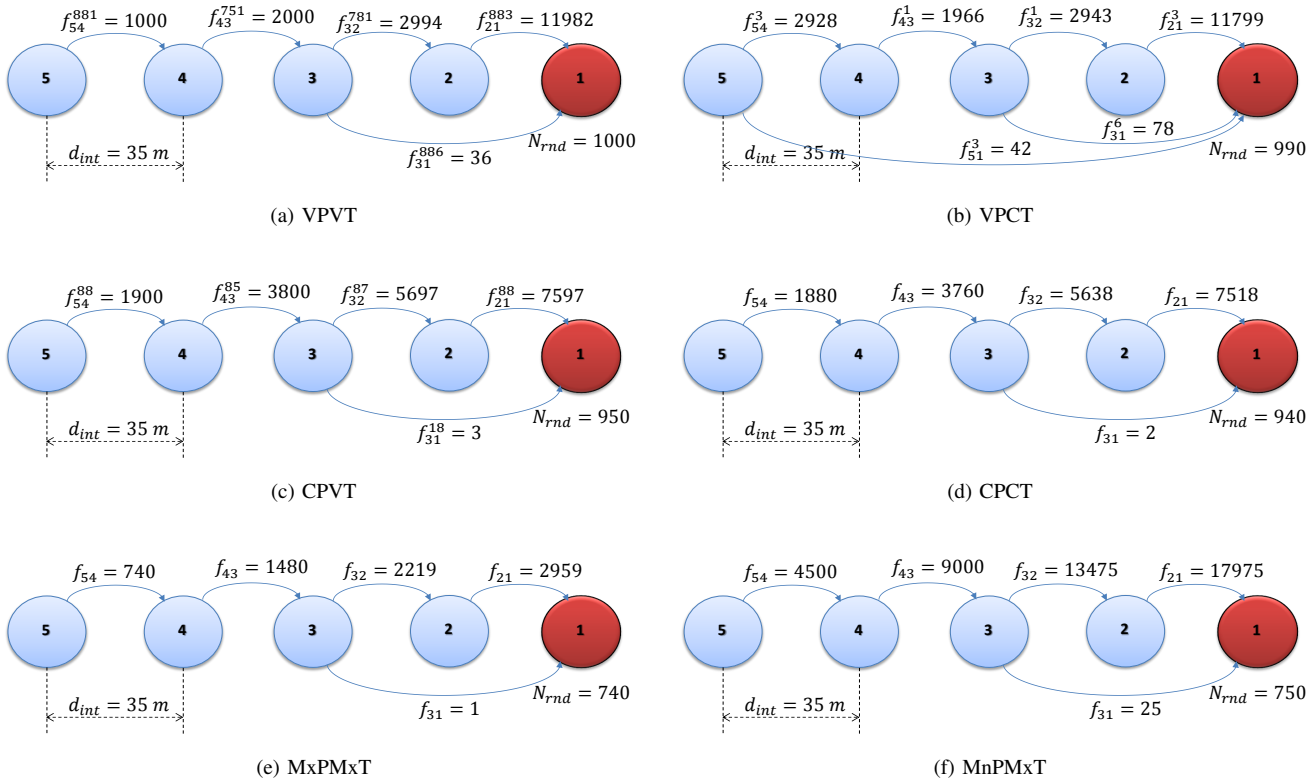

(a) VPVT (b) VPCT (c) CPVT (d) CPCT (e) MxPMxT (f) MnPMxT

Fig. 1: Normalized flows in a five-node line network (toy example) with OUS-L channel model.

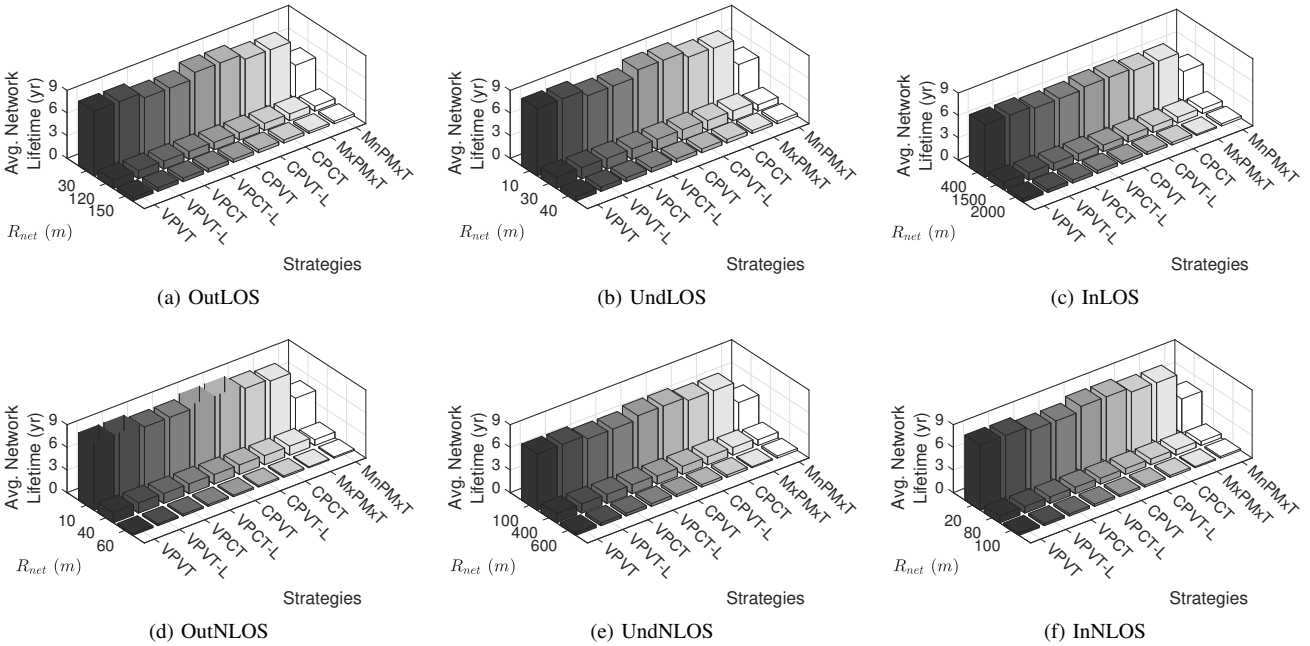

(a) OutLOS (b) UndLOS (c) InLOS (d) OutNLOS (e) UndNLOS (f) InNLOS

Fig. 2: Average NLs (in years) as a function of R_{net} for all strategies.

decision in prolonging NL under such conditions. However, due to the probabilistic nature of the propagation models, a small fraction of the links can exhibit much higher path loss values which is the reason for the average DPSs are not always 120 Bytes in densest networks. Even in the sparsest networks the average DPS for VPVT is not the lowest DPS allowable (*i.e.*, 20 Bytes), instead, the lowest utilized DPSs are approximately half of the maximum DPS (*e.g.*, 59.3 Bytes).

In densest network deployments in all SG environments NLs of the four main strategies, from highest to lowest, are

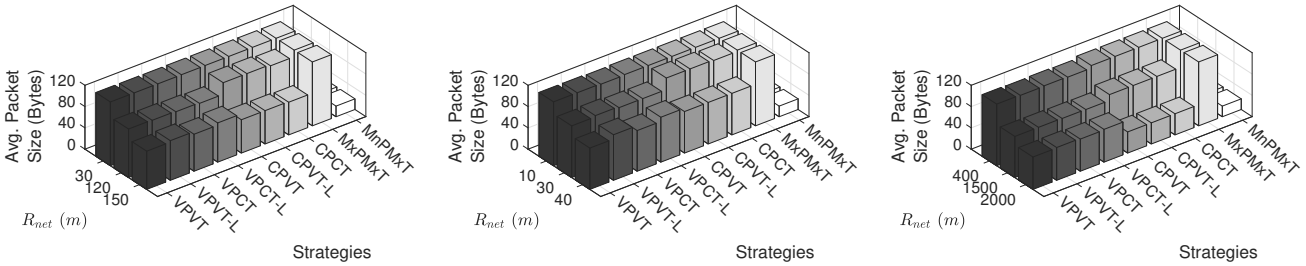

(a) OutLOS (b) UndLOS (c) InLOS

(d) OutNLOS (e) UndNLOS (f) InNLOS

Fig. 3: Average packet sizes (in Bytes) for all strategies as a function of R_{net} for all strategies.

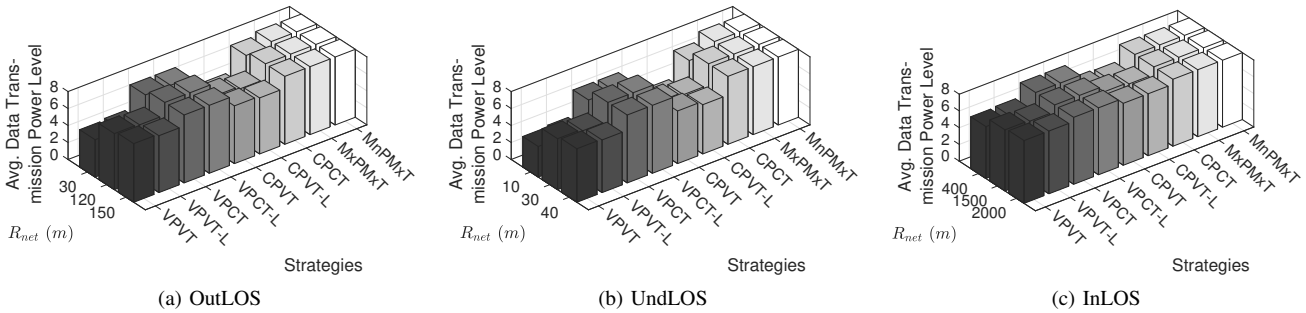

(a) OutLOS (b) UndLOS (c) InLOS

(d) OutNLOS (e) UndNLOS (f) InNLOS

Fig. 4: Average data TPLs as a function of R_{net} for all strategies.

obtained as VPVT, CPVT, VPCT, and CPCT. On the other hand, highest NLs in sparser deployments are obtained, from highest to lowest, as VPVT, VPCT, CPVT, and CPCT. In fact, the highest and lowest NL differences between VPVT and VPCT are 9.85% (OutNLOS, $R_{net} = 10$ m) and less than 0.01% (UndLOS, $R_{net} = 60$ m), respectively. NL differences between VPVT and CPCT are in the range of less than 0.01% (for all of the densest deployments) and 17.27% (UndLOS, $R_{net} = 60$ m). The minimum NL difference between VPVT and CPCT is 6.1% (UndLOS, $R_{net} = 10$ m) and the maximum difference is 19.39% (UndNLOS, $R_{net} = 60$ m). CPVT, VPCT, and CPCT strategies perform best when the average values of their DPSs and TPLs are closest to VPVT.

All three strategies using different link-level decision mechanisms (VPVT-L, VPCT-L, and CPVT-L) perform generally well when compared to their centralized counterparts. The difference between VPCT and VPCT-L is always less than 0.1%, likewise, the difference between CPVT and CPVT-L is, at most, 0.29% (InNLOS, $R_{net} = 20$ m). In the majority of the scenarios the difference between VPVT and VPVT-L is less

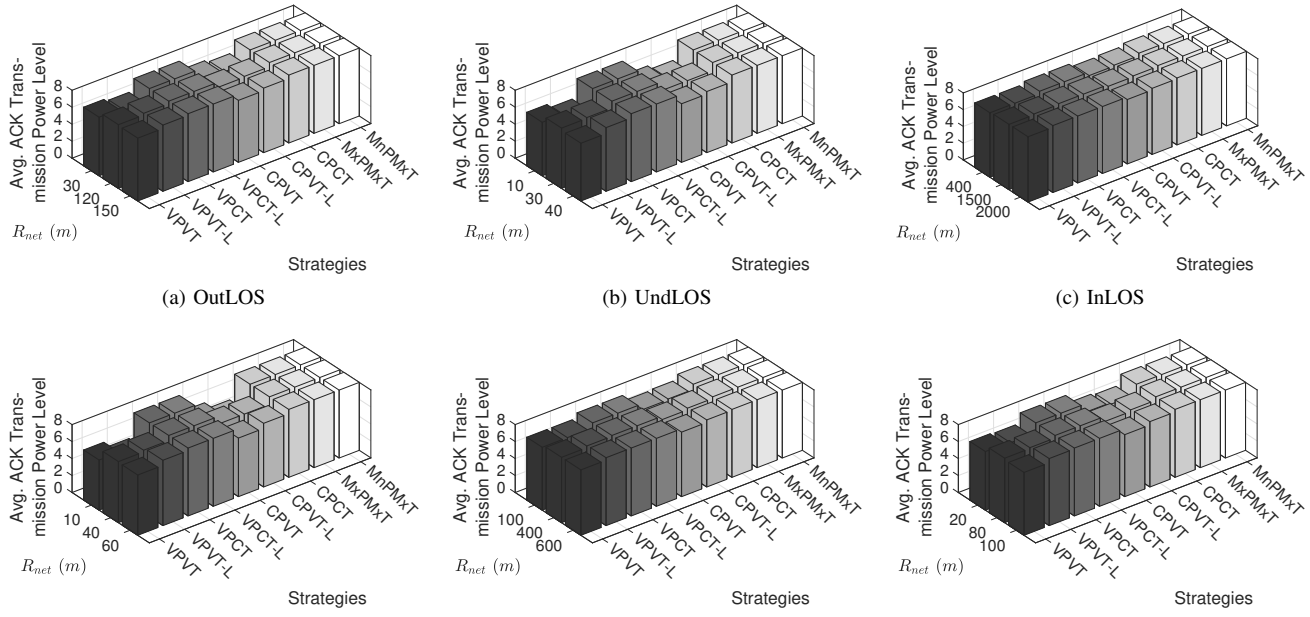

(a) OutLOS (b) UndLOS (c) InLOS

(d) OutNLOS (e) UndNLOS (f) InNLOS

Fig. 5: Average ACK TPLs as a function of R_{net} for all strategies.

than 0.3%, however, in some sparsest networks the difference becomes higher (*e.g.*, 4.11% for InLOS, $R_{net} = 600$ m).

Up to this point, we analyzed seven strategies utilizing certain DPS and TPL optimization mechanisms, however, in many protocols utilized in practice, DPS and TPLs are predetermined and fixed. MxPMxT and MnPMxT strategies exemplify such protocols. Both of these strategies perform significantly worse than the VPVT strategy. For example, MxPMxT and MnPMxT NLs are 61.54% (UndLOS, $R_{net} = 2000$ m) and 50.48% (UndNLOS, $R_{net} = 10$ m) lower than VPVT, respectively. Furthermore, these two strategies are outperformed by all other strategies in most of our scenarios.

VI. Conclusion and Future Research Directions

Our major novel contributions are enumerated as follows

1) We designed the VPVT strategy for link-level optimization of DPSs and data/ACK TPLs in WSNs employed in SG environments. Indeed, VPVT is the first strategy proposed in WSN literature that jointly optimizes TPL and DPS for each link to maximize WSN NL. Comparative evaluations of VPVT strategy against eight other strategies which are representatives of the models in the literature reveal the superior performance of VPVT.
2) We designed and compared the performances of four centralized strategies which optimize DPS and/or data/ACK TPLs by using link-level or network-level mechanisms (VPVT, VPCT, CPVT, and CPCT). The results of our analysis clearly show that link-level optimization of DPS and data/ACK TPLs significantly outperforms the network-level optimization. Therefore, there is a significant margin of improvement in terms of NL by utilizing link-level DPS and TPL optimization.
3) Differences between NLs obtained with the centralized and localized strategies (VPVT-L, VPCT-L, and CPVT-L) are negligibly low in most cases, therefore, our centralized strategies can be implemented as distributed algorithms without significant performance losses.

Future research directions are enumerated as follows:

1) It is possible to extend the framework presented in this study to other environments and platforms that we do not consider. Indeed, after obtaining the n, σ, and P_n values for the target environment, these values can directly be fed into the model. It is also possible to modify our model by updating Eqs. (17)–(19) and Table I according to the characteristics of the transceiver to be used.
2) Implementing strategies other than the ones we consider is also possible by modifying Eqs. (1)–(16). For example, if a multiple base station network is considered then it is sufficient to modify Eq. (2).
3) Design and characterization of distributed WSN protocols that optimize TPL and DPS jointly for each link is a promising open research area.

References

[1] V. C. Gungor, D. Sahin, T. Kocak, S. Ergut, C. Buccella, C. Cecati, and G. P. Hancke, "Smart grid technologies: Communication technologies and standards," *IEEE Trans. Ind. Informat.*, vol. 7, no. 4, pp. 529–539, Nov 2011.

[2] M. H. Cintuglu, O. A. Mohammed, K. Akkaya, and A. S. Uluagac, "A survey on smart grid cyber-physical system testbeds," *IEEE Commun. Surveys Tut.*, vol. 19, no. 1, pp. 446–464, First Quarter 2017.

[3] A. A. Khan, M. H. Rehmani, and M. Reisslein, "Requirements, design challenges, and review of routing and MAC protocols for CR-based smart grid systems," *IEEE Commun. Mag.*, vol. 55, no. 5, pp. 206–215, May 2017.

[4] N. Saputro, K. Akkaya, and S. Uludag, "A survey of routing protocols for smart grid communications," *Comput. Netw.*, vol. 56, no. 11, pp. 2742–2771, Jul 2012.

[5] V. C. Gungor, B. Lu, and G. P. Hancke, "Opportunities and challenges of wireless sensor networks in smart grid," *IEEE Trans. Ind. Electron.*, vol. 57, no. 10, pp. 3557–3564, Oct 2010.

[6] S. Kurt, H. U. Yildiz, M. Yigit, B. Tavli, and V. C. Gungor, "Packet size optimization in wireless sensor networks for smart grid applications," *IEEE Trans. Ind. Electron.*, vol. 64, no. 3, pp. 2392–2401, Mar 2017.

[7] S. Kurt and B. Tavli, "Path-loss modeling for wireless sensor networks: A review of models and comparative evaluations." *IEEE Antennas Propag. Mag.*, vol. 59, no. 1, pp. 18–37, Feb 2017.

[8] M. Yigit, S. Kurt, H. U. Yildiz, B. Tavli, and V. C. Gungor, "A survey on packet size optimization for terrestrial, underwater, underground, and body area sensor networks," *Int. J. Commun. Syst.*, vol. 31, no. 11, p. e3572, Jul 2018.

[9] N. Pantazis and D. Vergados, "A survey on power control issues in wireless sensor networks," *IEEE Commun. Surveys Tut.*, vol. 9, no. 4, pp. 86–107, Fourth Quarter 2007.

[10] H. Cotuk, B. Tavli, K. Bicakci, and M. B. Akgun, "The impact of bandwidth constraints on the energy consumption of wireless sensor networks," in *Proc. IEEE Wireless Commun. and Netw. Conf. (WCNC)*, Apr 2014, pp. 2787–2792.

[11] H. U. Yildiz, B. Tavli, and H. Yanikomeroglu, "Transmission power control for link-level handshaking in wireless sensor networks," *IEEE Sensors J.*, vol. 16, no. 2, pp. 561–576, Jan 2016.

[12] M. Barcelo, A. Correa, J. L. Vicario, and A. Morell, "Joint routing and transmission power control for collection tree protocol in WSN," in *Proc. IEEE Int. Symp. Personal Indoor and Mobile Radio Commun. (PIMRC)*, Dec 2013, pp. 1989–1993.

[13] W. B. Pottner and L. Wolf, "Probe-based transmission power control for dependable wireless sensor networks," in *Proc. IEEE Int. Conf. Distrib. Comput. Sensor Syst. (DCOSS)*, Jul 2013, pp. 44–51.

[14] O. Cayirpunar, E. Kadioglu-Urtis, and B. Tavli, "Optimal base station mobility patterns for wireless sensor network lifetime maximization," *IEEE Sensors J.*, vol. 15, no. 11, pp. 6592–6603, Nov 2015.

[15] S. Lin, F. Miao, J. Zhang, G. Zhou, L. Gu, T. He, J. A. Stankovic, S. Son, and G. J. Pappas, "ATPC: Adaptive transmission power control for wireless sensor networks," *ACM T. Sensor Netw.*, vol. 12, no. 1, pp. 6:1–6:31, Mar 2016.

[16] I. Bennis, M. Ayaida, M. Herbin, and F. Blanchard, "Link-gain based power control mechanism for wireless sensor networks," in *Proc. Int. Wireless Commun. and Mobile Comput. Conf. (IWCMC)*, Jun 2017, pp. 1413–1418.

[17] M. Holland, T. Wang, B. Tavli, A. Seyedi, and W. Heinzelman, "Optimizing physical-layer parameters for wireless sensor networks," *ACM T. Sensor Netw.*, vol. 7, no. 4, pp. 28:1–28:20, Feb 2011.

[18] S. Abdulhadi, M. Naeem, M. Jaseemuddin, and A. Anpalagan, "Optimized packet size for energy efficient cooperative wireless ad-hoc networks," in *Proc. IEEE Int. Conf. Commun. Workshops (ICC)*, Jun 2013, pp. 581–585.

[19] W. Dong, X. Liu, C. Chen, Y. He, G. Chen, Y. Liu, and J. Bu, "DPLC: Dynamic packet length control in wireless sensor networks," in *Proc. IEEE Conf. Comput. Commun. (INFOCOM)*, Mar 2010, pp. 1–9.

[20] K. Lendvai, A. Milankovich, S. Imre, and S. Szabo, "Optimized packet size for energy efficient delay-tolerant sensor networks," in *Proc. IEEE Int. Conf. Wireless and Mobile Comput. Netw. Commun. (WiMob)*, Oct 2012, pp. 19–25.

[21] A. Jamal, C. Tham, and W. Wong, "Dynamic packet size optimization and channel selection for cognitive radio sensor networks," *IEEE Trans. Cogn. Commun. Netw.*, vol. 1, no. 4, pp. 394–405, Dec 2015.

[22] A. Akbas, H. U. Yildiz, B. Tavli, and S. Uludag, "Joint optimization of transmission power level and packet size for WSN lifetime maximization," *IEEE Sensors J.*, vol. 16, no. 12, pp. 5084–5094, Jun 2016.

[23] X. Wang, X. Wang, G. Xing, and Y. Yao, "Minimum transmission power configuration in real-time sensor networks with overlapping channels," *ACM T. Sensor Netw.*, vol. 9, no. 2, pp. 10:1–10:28, Apr 2013.

[24] J. Jeong, D. Culler, and J. H. Oh, "Empirical analysis of transmission power control algorithms for wireless sensor networks," in *Proc. Int. Conf. Networked Sensing Systems (INSS)*, Sep 2007, pp. 27–34.

[25] M.-A. Koulali, A. Kobbane, M. El Koutbi, H. Tembine, and J. Ben-Othman, "Dynamic power control for energy harvesting wireless multimedia sensor networks," *EURASIP J. Wireless Commun. and Netw.*, vol. 2012, no. 1, pp. 158:1–158:8, May 2012.

[26] R. Srivastava and C. Koksal, "Energy optimal transmission scheduling in wireless sensor networks," *IEEE Trans. Wireless Commun.*, vol. 9, no. 5, pp. 1550–1560, May 2010.

[27] A. Nandi, D. Bepari, and S. Kundu, "Optimal transmit power and packet size in wireless sensor networks in shadowed channel," *ACEEE Int. J. Commun.*, vol. 1, no. 2, pp. 39–44, Jul 2010.

[28] S. Basagni, C. Petrioli, R. Petroccia, and M. Stojanovic, "Optimized packet size selection in underwater wireless sensor network communications," *IEEE J. Ocean. Eng.*, vol. 37, no. 3, pp. 321–337, Jun 2012.

[29] Z. Ning, X. Wang, X. Kong, and W. Hou, "A social-aware group formation framework for information diffusion in narrowband internet of things," *IEEE Internet Things J.*, vol. 5, no. 3, pp. 1527–1538, Jun 2018.

[30] Z. Ning, F. Xia, X. Hu, Z. Chen, and M. S. Obaidat, "Social-oriented adaptive transmission in opportunistic internet of smartphones," *IEEE Trans. Ind. Informat.*, vol. 13, no. 2, pp. 810–820, Apr 2017.

[31] (2018) Tmote Sky datasheet. [Online]. Available: http://www.snm.ethz.ch/snmwiki/pub/uploads/Projects/tmote_sky_datasheet.pdf

[32] I. Demirkol, C. Ersoy, and F. Alagoz, "MAC protocols for wireless sensor networks: a survey," *IEEE Commun. Mag.*, vol. 44, no. 4, pp. 115–121, Apr 2006.

[33] M. Zuniga and B. Krishnamachari, "Analyzing the transitional region in low power wireless links," in *Proc. IEEE Commun. Society Conf. Sensor and Ad Hoc Commun. and Netw. (SECON)*, Oct 2004, pp. 517–526.

Huseyin Ugur Yildiz (S'13-–M'16) received the B.S. degree from Bilkent University, Ankara, Turkey, in 2009, and the M.S. and Ph.D. degrees from TOBB University of Economics and Technology, Ankara, Turkey, in 2013 and 2016, respectively, all in electrical and electronics engineering. He is an Assistant Professor in the Department of Electrical and Electronics Engineering at TED University, Ankara, Turkey. His research focuses on the applications of optimization techniques for modeling and analyzing research problems on wireless communications, wireless networks, underwater acoustic networks, and smart grids.

Sinan Kurt received his BS and MS degrees in Electrical and Electronics Engineering from the Middle East Technical University, Ankara, Turkey, in 2004 and 2007, respectively. He received his PhD degree in Electrical and Electronics Engineering, from the TOBB University of Economics and Technology, Ankara, Turkey, in 2016. His research interests lie in the areas of wireless communications, electromagnetics, circuit design, wireless networks, and optimization.

Bulent Tavli (S'97—M'05–SM'17) is a Professor at the Electrical and Electronics Engineering Department, TOBB University of Economics and Technology, Ankara, Turkey. He received his BS degree in Electrical and Electronics Engineering from the Middle East Technical University, Ankara, Turkey, in 1996. He received his MS and PhD degrees in Electrical and Computer Engineering from the University of Rochester, Rochester, NY, USA in 2002 and 2005, respectively. Wireless communications, networking, optimization, embedded systems, information security, smart grid, and blockchain are his current research areas.